molecular pharmaceutics

ARTICLE

pubs.acs.org/molecularpharmaceutics

Atomistic Simulation and Measurement of pH Dependent Cancer Therapeutic Interactions with Nanodiamond Carrier

Ashfaq Adnan,[†] Robert Lam,[‡] Hanning Chen,[§] Jessica Lee,[‡] Daniel J. Schaffer,[∥] Amanda S. Barnard,[#] George C. Schatz,[§,∥] Dean Ho,[‡,⊥,▽] and Wing Kam Liu*[,▽,○]

[†]Department of Mechanical & Aerospace Engineering, University of Texas, Arlington, Texas 76019, United States

[‡]Department of Biomedical Engineering, Northwestern University, Evanston, Illinois 60208, United States

[§]Department of Chemistry, Northwestern University, Evanston, Illinois 60208, United States

[∥]Chemical and Biological Engineering, Northwestern University, Evanston, Illinois 60208, United States

[⊥]Robert H. Lurie Comprehensive Cancer Center, Northwestern University, Chicago, Illinois 60611, United States

[#]CSIRO Materials Science and Engineering, Clayton, Victoria 3168, Australia

[▽]Department of Mechanical Engineering, Northwestern University, Evanston, Illinois 60208, United States

ABSTRACT: In this work, we have combined constant-pH molecular dynamics simulations and experiments to provide a quantitative analysis of pH dependent interactions between doxorubicin hydrochloride (DOX) cancer therapeutic and faceted nanodiamond (ND) nanoparticle carriers. Our study suggests that when a mixture of faceted ND and DOX is dissolved in a solvent, the pH of this solvent plays a controlling role in the adsorption of DOX molecules on the ND. We find that the binding of DOX molecules on ND occurs only at high pH and requires at least ∼10% of ND surface area to be fully titrated for binding to occur. As such, this study reveals important mechanistic insight underlying an ND-based pH-controlled therapeutic platform.

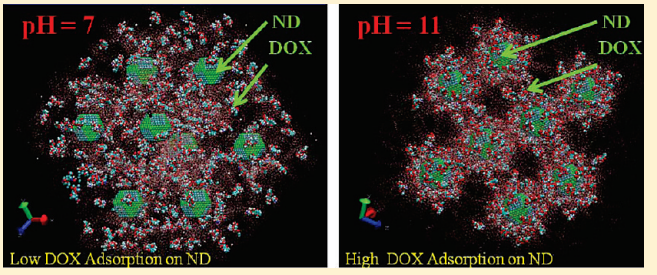

KEYWORDS: nanodiamond, CpHMD, doxorubicine, adsorption, drug delivery

1. INTRODUCTION

Recently there has been important progress in the development of nanodiamonds (NDs) as carriers for a variety of biologically applicable agents[1−4] due to their exceptional biocompatibility[1,5,6] and unique surface properties.[7−9] Through adsorption, a variety of agents have been shown to reversibly bind and unbind from the ND surface as conditions were altered from basic to acidic, respectively. In addition, the bioagents were observed to coat and/or were entrapped between ND aggregates, possibly indicating a capacity for therapeutic sequestration. This "shielding" effect suggests inherent protection against nonspecific perturbations, a feature shown in clinically available alternatives for reducing side effects such as alopecia and nausea.[10,11]

This dynamic interaction between drugs and NDs has also led to exploration with water-insoluble compounds,[4] as several systemically administered drugs are limited by aqueous solubility.[12] After combining these drugs with NDs, there was a 3 order of magnitude decrease in drug aggregate size to on the order of ∼100 nm,[4] suggesting that NDs can facilitate greater drug solubility within aqueous solutions. ND-based gene delivery has demonstrated a 70 times enhancement to delivery efficacy compared with a commercial standard.[13] In addition, a spectrum of studies pertaining to single-cell ND injection,[14] ND-based micro/nanofilm approaches for localized drug release[15,16] and ND-based magnetic resonance imaging[17] have further revealed their broad applicability in biology and medicine.

While experimental results demonstrating these effects have established the potential of NDs as versatile therapeutic platforms, the underlying atomic and nanoscale mechanisms of drug adsorption and release remain challenging to ascertain. In this study, atomistic computer simulations have been used to analyze the underlying mechanisms behind drug adsorption onto NDs. Study of this process requires fundamental analysis of surface charge, chemical analysis and drug adsorption and desorption dynamics. Toward this end, the simulation results are verified experimentally with UV−vis spectroscopy, dynamic light scattering, and centrifugation based assays.

Within this simulation framework, doxorubicin hydrochloride (DOX), a common apoptotic chemotherapeutic, was used as a

Received: July 19, 2010
Accepted: December 20, 2010
Revised: November 2, 2010
Published: December 20, 2010

model agent. It was previously demonstrated that DOX and ND interact only weakly under ambient conditions due to low aqueous solubility.[1] Sustained ND−drug interactions were mediated by adding salts or increasing the solvent basicity.[1] The significant role of pH in facilitating the interactions between DOX and the ND surfaces provides a platform upon which atomistic simulations were designed in this study to further examine the DOX−ND interaction.

Due to recent work by Barnard,[7] Sternberg[8] and Osawa et al.,[9] a theoretical model for the electrostatic potential of unfunctionalized ND has been developed. Density functional tight binding-based simulations indicate that the interparticle interactions between NDs depend on charges on the surface facets, leading to preferentially ordered self-assembled ND agglutinates.[7,8] For the functionalized NDs used for drug binding, it is the ionizable groups on the ND surface, rather than the intrinsic ND electrostatics, that dominate the interaction with charged drug molecules like DOX. Indeed, experiments show that the ND−DOX equilibrium can be shifted by varying pH,[1] so in this work we develop a model for the variation of surface charge with pH, and then use molecular dynamics simulations to determine the drug loading properties.

There have been a few earlier studies of the binding of biomolecules to diamond surfaces. One is Larsson's work concerning the binding of bone morphogenetic protein-2 to nanocrystalline diamond (which is relevant to the use of diamond in medical implants).[18,19] In this work the primary interest was on the hydrophilic environment associated with an OH covered diamond surface as this results in stronger interactions with the protein than the hydrophobic environment associated with hydrogen terminated diamond. pH effects were not studied so the role of acid/base equilibria on binding was not considered. Related results were obtained by Netz and co-workers, and by Borisenko et al., who studied polypeptides and proteins interacting with hydrophobic and hydrophilic diamond surfaces.[20−22]

2. PH CONTROLLED ND−DOX INTERACTIONS

2.1. Atomistic Simulations. Here we have adopted a constant pH molecular dynamics simulation (CpHMD) technique to explore the pH dependent interactions between DOX and ND. This method is a simplified version of the method of Baptista et al.[23] The atomistic model we chose is shown in Figure 1, with detailed structures of the ND and DOX given in Figure 2. This model consists of a single ND plus several DOX molecules, counterions and water molecules. A truncated octahedral ND with a diameter of 3.5 nm is chosen to provide a structure that is probably typical of nonaggregated ND. This ND has 1880 carbon atoms, 8 (111) facets and 6 (100) facets, such that there are 53 atoms per (111) facet and 55 atoms per (100) facet. In order to see the effect of scaling, we have also studied another set of models that contains eight uniformly dispersed NDs and proportional amounts of DOX, counterions and solvent molecules compared to the smaller system we described above. The size of the larger model is precisely maintained eight times larger than the smaller model.

Although we use a bare ND in our modeling, the properties of the surface carbon atoms are modified to reflect functionalization whose properties are only poorly known. Some "possible" functional groups for ND have been identified as −COOH, −CONH, −OH, −CO, $-NH_2$, −SH, $-CH_2$, −H etc.[24] However, the exact types and percent coverage of these functional groups on ND surfaces are not yet known. In our study, we have assumed

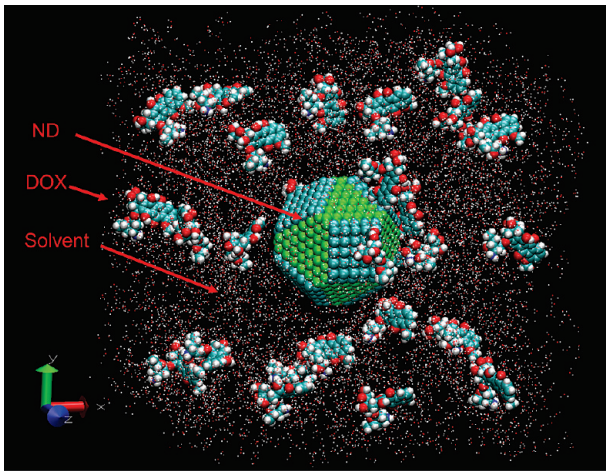

Figure 1. Initial structure of atomistic model of ND−DOX−solvent (pH buffer) system that is simulated via MD to study the pH dependent ND−DOX binding. In the solvent media, twenty-six DOX molecules are allowed to interact with one truncated octahedral ND particle that is functionalized (30% of total ND surface area). The surface electrostatics on the ND surface depends on the pH of the solvent. Here the green and cyan color on ND refer to the atoms belonging to (111) and (100) facets, respectively.

that the ND surface is coated with "some" ionizable species such that the dominant interaction with DOX is determined by the pH dependent electrostatics in which the charge state of the surface carbons is adjusted based on an assumed pK_a and an assumed maximum ionization density. In reality, the overall pK_a of the ND will depend on the pK_a of all individual functional groups. Therefore, our model may be considered as an "effective" model where the overall pK_a of ND is chosen from experimental observation and the local pK_a's of individual functional groups have been smeared into a single pK_a.

The CpHMD calculation is essentially a conventional MD simulation that is coupled with a stochastic protonation/deprotonation algorithm to take into account the variation in the protonation equilibrium of the titratable surface sites on the ND and the amine group on the DOX as determined by solvent pH. The fraction of sites on the ND or DOX that are charged is determined as a function of pH by the Henderson−Hasselbalch relation.[25−27] Thus if x refers to the fraction of protonated (deprotonated) sites, then the Henderson−Hasselbalch relation[25−27] suggests that the number of sites $N_{charged}$ out of N_{total} sites that can be charged at a certain pH is

$$\begin{aligned} pK_a &= pH + \log_{10}\left(\frac{x}{1-x}\right) \\ \Rightarrow x &= \frac{10^{pK_a - pH}}{1 + 10^{pK_a - pH}} = \frac{N_{charged}}{N_{total}} \\ \Rightarrow N_{charged} &= \frac{10^{pK_a - pH}}{1 + 10^{pK_a - pH}} N_{total} \end{aligned} \quad (1)$$

N_{total} refers to the total number of "titratable" or "ionizable" sites available for a particular molecule. For ND, the nature and density of ionizable species is not known, so we simply assume that some fraction of the surface carbons can be ionized. While it is geometrically possible to functionalize every ND surface atom with such functional groups, in reality, repulsions between these groups would create tremendous instability. Thus we have assumed

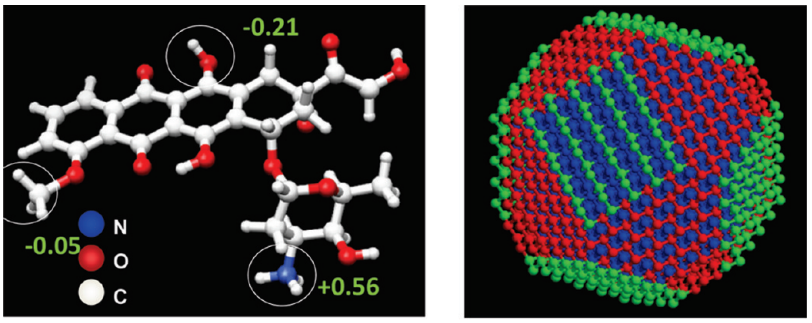

Figure 2. Atomistic models for (a) DOX and (b) truncated octahedral ND nanoparticle. Note that DOX molecules contain primarily OH, CH_3 and NH_3 side groups on their backbone; the partial charges of these side groups, as predicted from combined DFTB-SCC and RESP calculations, vary substantially: both by magnitude and by sign. Some representative charges are shown in (a) in elementary charge units. The ND surface contains eight {111} facets (hexagonal and colored red) and six {100} facets (square and colored green). All atoms of ND are C atoms. Here the core atoms are colored in blue for clarity.

that the functional groups are separated by at least one nearest neighbor. Based on the packing of functional groups on the ND surface, we estimate that the maximum N_{total} can be 30% of the total number of carbon atoms available on ND surface. Later we will test the sensitivity of our results to this assumption pertaining to maximum surface charge density.

In our simulations, we determined $N_{charged}$ by assuming that the pK_a of the ND is 10.75.[28] We have estimated this pK_a value based on the *isoelectric point* (IEP)[29] in the zeta potential vs pH plot reported in the literature[28] and also based on our own experimental observations.[3] This procedure potentially integrates several acid−base equilibrium processes into a single effective ionization step. Once we set the pK_a for ND, we have then estimated the N_{charge} from eq 1 and randomly located these deprotonated sites on the ND surface. This is different from the case of ND in the absence of functionalization, where the charge distribution is facet dependent. The electrostatic charges for the functional sites are defined by assigning partial charges to the chosen sites (−1 elementary charge) while the remaining ND surface atoms are kept neutral (0 elementary charge). This implicitly assumes that the ionizable species is neutral at low pH and becomes negative at high pH, however it is also compatible with acid/base equilibria (like OH groups) which are positive at low pH and neutral at high pH provided that we also assume that the particle has a net charge such that it is neutral at low pH.

The electrostatic charges for the DOX molecules are developed from the restrained electrostatic potential method (RESP)[30] by fitting the quantum mechanics electrostatics potential (based on DFTB-SCC[7]) under the constraints of fixed total charge for the whole system or its fragments. In this calculation, the initial structure for DOX has been obtained from the Protein Data Bank. In our study, we assumed pK_a for DOX is 8.3.[36] This implies that DOX remains neutral at high pH and is charged at low pH. At any intermediate pH, some of the DOX molecules will be protonated and some of them will not, and the percentage of protonated DOX will depend on their pK_a as determined by eq 1. For instance, at pH = 8.3, 50% of the DOX are protonated.

As shown in Figure 1, the initial configuration consists of one ND and twenty-six DOX molecules that are solvated with 6200 SPC water molecules in a simulation box of dimensions $L_x = L_y = L_z = 9.0$ nm. The ND and DOX were modeled with the Tersoff[31] and DREIDING potentials,[32] respectively. The ND−DOX interactions were modeled by nonbonded Lennard-Jones (LJ) potential[33] in addition to the pH dependent electrostatic/coloumbic interactions. The appropriate parameters (σ and ε for LJ potential) for the ND−DOX nonbonded interactions were obtained by using the method described in ref 32.

Periodic boundary conditions for the electrostatic interaction are defined by the EWALD summation method, and VDW interactions are defined by a LJ potential.[33] All simulations were performed at 300 K with a Nosé−Hoover based canonical ensemble.[34] To balance the overall system charge that arises due to the presence of a large number of negatively charged sites on ND, an appropriate number of positively charged sodium ions (+1 elementary charge) were randomly added in the excluded volume (i.e., the solvent) of the MD model. A similar procedure has been adopted for the larger model that contains 8 NDs, 208 DOX molecules, 49600 SPC water molecules and appropriate number of counterions. The dimensions of the large simulation box are $L_x = L_y = L_z = 18.0$ nm.

MD simulations at various pH levels have been performed for pH in the range from 6 to 11 with an interval of 0.5. For each pH level, the MD simulations are run for up to 100 ps and the DOX−ND interactions are monitored. To quantify DOX binding to the ND, the minimum distance between the NH_2 site on DOX and the nearest ND facet is calculated. A DOX molecule is considered territorially bound to ND if this distance is 3.5 Å or less. The choice of this critical distance is based on the VDW separation distance between C atoms and N atoms.

2.2. Materials and Methods: Doxorubicin−Nanodiamond pH Adsorbance Test. 100 μg of doxorubicin (US Pharmacopeia, Rockville, MD) was vortexed briefly with 500 μg of sonicated nanodiamonds (Nanocarbon Research Institute, Japan) in a buffer of variable pH. Buffer pH was calculated via pH probe after hydrochloric acid (Sigma Aldrich) and sodium hydroxide (Sigma Aldrich) additions. Vials were then centrifuged at 14,000 rpm for 5 min to pellet the nanodiamonds, and supernatant was subsequently analyzed for UV−vis absorbance at 484 nm. Standard curves were utilized to determine drug concentration as a function of absorbance. This experiment was performed with ten independent replicates and the standard deviation and standard error about the mean calculated.

3. RESULTS AND DISCUSSION

Prior to conducting the pH dependent study, we first determined the maximum binding capacity of DOX molecules on the

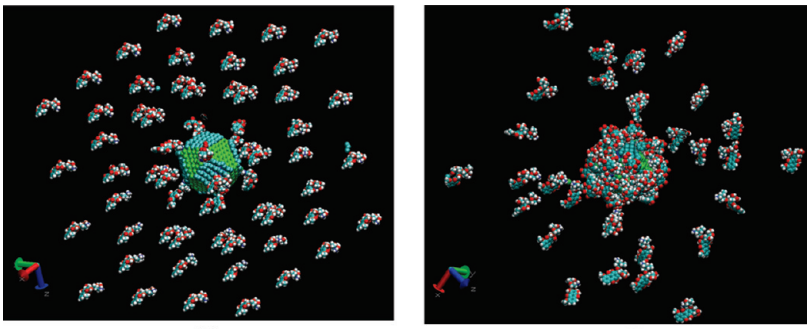

Figure 3. DOX loading saturation simulations. Sixty-four DOX molecules are allowed to interact with fully titrated ND (30% ND surface area is charged). MD snapshots are taken at 5 ps (a) and 100 ps (b), respectively. The saturation of DOX on the ND occurs when DOX molecules fully occupy the ND surface. In this situation, even though the ND has available sites for DOX attachment, the DOX cannot attach on the ND because they cannot penetrate through already bound DOX molecules (steric crowding).

ND. For this, we performed MD simulations with one ND and 64 DOX molecules in solvent for 100 ps. The surface of the ND is assumed to be functionalized with 30% ionizable sites, and all of these sites are fully titrated (charged) corresponding to the high pH limit. Figure 3 shows two snapshots taken at 5 and 100 ps, respectively. This shows that not all 64 DOX molecules can bind to the ND, even though the charge density is quite high. Instead we find that a maximum of 26 DOX molecules can bind. The remaining DOX molecules are found to be somewhat attracted to ND but fail to territorially bind with the ND primarily because of steric crowding. Since there are a total of 14 facets on the ND, we find that roughly two DOX per facet can bind. Based on these findings, we included 26 DOX molecules in our pH dependent calculations. This corresponds to a DOX concentration that is 0.06 M, obviously much higher than what is practical experimentally, which means that our binding estimates will serve as upper bounds. It is believed that the extent of steric crowding largely depends on the ND size (mostly the facet size) and DOX cross-section (the DOX "footprint" area occupied per ND facet area). Therefore, exactly how many DOX molecules can attach per ND facet will vary substantially with the change in ND size. For the larger model that has 8 NDs, we included 208 DOX in the system so that the DOX to ND ratio remains consistent.

Figure 4 shows final MD snapshots (after 100 ps) of the ND−DOX system (ND with 30% functional group) at different pH levels. Note that, at the beginning of the simulation, the drug molecules are located at least 15 Å from the ND surface. Figure 4 shows that, at lower pH, the DOX molecules do not bind to the ND; rather they maintain a stable separation from the ND surface. This happens because, at lower pH, most of the ND surface atoms are neutral and their electrostatic interactions with DOX are not strong enough. At high pH, the electrostatic interactions become stronger, leading to more DOX molecules bound to the ND surface.

To quantify exactly how many ionizable sites are required on each ND facet to bind a DOX, other sets of MD simulations have been performed where sites in one of the ND facets are incrementally assigned with charges (−1 elementary charge). We have performed a total of 10 MD simulations where the ND is allowed to interact with one DOX in the water solvent. We refer to these MD models as M1, M2, ... through M10 where the number following "M" represents the number of sites on the ND that are charged. In other words, the M1 model has one charged site, the M2 has two charged sites and so on. As before, the unbalanced charged in the system is neutralized by adding an appropriate number of Na^+ in the excluded volume of the solvent. In Figure 5, the final ND−DOX distance is shown for all 10 models. From this study, it can be observed that at least 5 sites are necessary per ND facet to ensure effective binding. This corresponds to about 10% of the ∼50 atoms available per facet, which thus provides a lower bound to the extent of surface functionalization that is needed for binding to occur. It also suggests that the observed maximum coverage of DOX noted above, namely, 2 DOX per facet, would correspond to about 20% surface functionalization. In order to understand the role of functional group amount on ND surface, we have studied three different percentages of functional group on ND surface, namely, 30%, 20% and 10%.

In Figure 6, MD simulation results for the number of drug adsorption per ND are plotted versus pH and have been compared with experimental results. As discussed earlier, we consider a DOX molecule to be bound to the ND surface when the amino group of the DOX maintains a van der Waals separation distance (<∼3.5 Å) from the ND. It can be observed that presence of 30% and 20% functional groups on ND surface has yielded similar results. For the 10% functional group case, the trend in results with respect to pH variation remains the same but the total number of DOX binding on ND surface is seen to be reduced substantially. These results suggest that 10% functional group coverage is not sufficient for maximum DOX binding on the ND we studied. On the other hand, the maximum DOX capacity on the ND was observed to be reached already with 20% functional group coverage. As a result 30% functional group presence on the ND surface is more than necessary for maximum DOX binding.

In Figure 6, we present simulation results for the large model (contains 8 ND and 208 DOX). For each of the ND surfaces of this model, 30% of the surface was covered with functional groups. It can be seen from Figure 6 that the number of DOX bound per ND at the different pH levels agrees quite well with the small model results. It can be inferred from these comparisons that the effect of simulation length scale is not critical for this particular study.

Figure 6 also presents a comparison of our calculated results with experiments that we have performed. Experimentally, UV−vis spectral analysis was performed to measure DOX adsorption capacity. 100 μg of doxorubicin (US Pharmacopeia, Rockville, MD) and 500 μg of sonicated nanodiamonds (Nanocarbon Research Institute, Japan) were mixed in a buffer

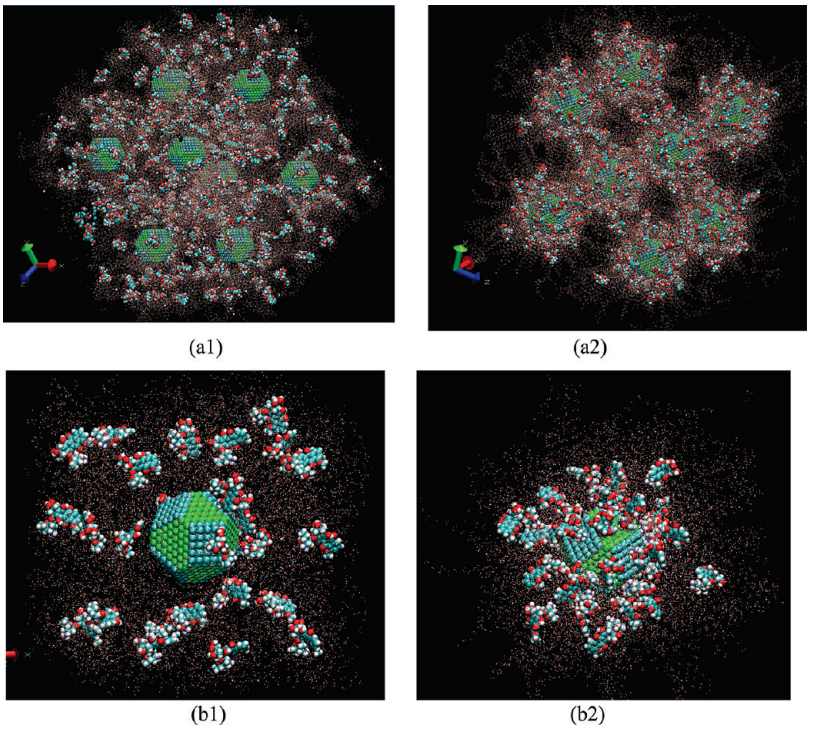

Figure 4. Representative final MD snapshots for the DOX−ND interaction simulation at different pH level: (a) large model with 8 NDs and 208 DOX in the solvent and (b) small model with 1 ND and 26 DOX in the solvent. The coverage of functional group is 30% of the ND surface. Panels a1 and a2 represent pH equal to 7 and 11, respectively. Panels b1 and b2 represent pH equal to 6.5 and 10.5, respectively. For clarity the water molecules are shown in point form whereas DOX and ND are shown in VDW sphere form. Different ND facets are shown in different colors. Note that at lower pH (pH < 8) only a few DOX molecules bind to ND, but at higher pH level (pH > 8), most are bound.

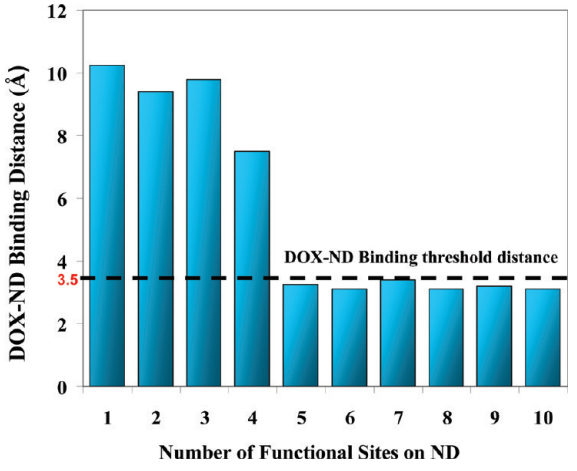

Figure 5. DOX−ND binding simulation study as function of number of binding sites available for one DOX molecules. Selected numbers of atoms in one of the ND facets have been assigned to −1 elementary electron charge to represent the number of functional sites on ND. This ND is allowed to interact with a DOX (initial separation between DOX and ND is about 1.5 nm) molecule in a solvent. Number of ND atoms assigned to charges varied from 1 to 10. For each simulation, the equilibrium distance between ND facet and DOX molecule is measured and plotted. It appears that at least 5 sites per ND facet are required to establish territorial binding of DOX with ND.

of variable pH. Adsorption capacities were calculated by comparing the UV−vis spectra of DOX remaining within the supernatant before and after centrifugation (1400 rpm, 2 h). Since DOX has a concentration dependent visible absorption peak around 484 nm, the amount of bound and unbound DOX can be inferred and calculated. Assuming that 10 mg of 5 nm diameter NDs contains 5.75×10^{16} nanoparticles (specifications provided by Nanocarbon Research Institute, Japan), the exact amount of DOX molecules adsorbed per nanoparticle can be measured.

It can be inferred from Figure 6 that our MD results qualitatively match the experimental findings of pH dependent drug adsorption capacity. Here we should note that the measured DOX coverage has been converted into a number of DOX molecules per particle by assuming that all the ND in the sample have a surface area that matches what we have assumed in the calculation. Obviously the transition between low coverage and high coverage depends on our assumed ND pK_a, so the match with experiment for this property is fixed by the model. However the maximum coverage in the calculations is not tied to the experiment yet it is seen to be similar to what we have estimated for the 20% or 30% functionalization models.

Discrepancies between experiment and simulation can be attributed to several factors. In reality the NDs may appear in other structural forms such as octahedral, cubooctahedral etc., and they might be functionalized with many other surface groups such as CH_3 etc. as outlined by Shenderova et al.[24] that might reduce the adsorption capacity compared to the calculations. The DOX concentration used in the MD simulations is well above that considered in the experiments, and moreover, depending on concentration, temperature and/or pH, DOX has been shown to associate into dimers and higher polymers through self-association in aqueous solution.[35] We have previously postulated that the ND surface charges are modified in response to the DOX

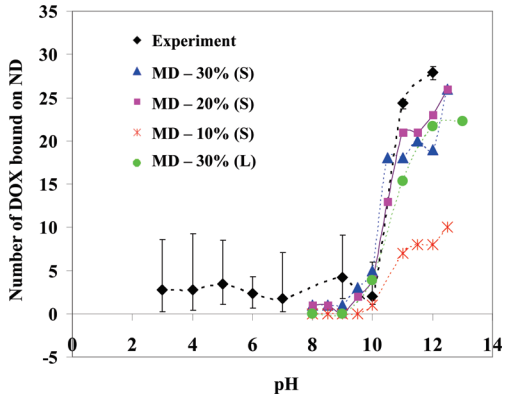

Figure 6. pH dependent DOX−ND binding capacity. At lower pH, few DOX molecules are adsorbed because of limited availability of titrated ND sites. At higher pH, enhanced adsorption is attributed to larger availability of titrated ND sites. For the smaller system (shown as "S" in the chart legend) MD simulations are performed for three different percentages of functional groups on the ND surface, namely, 30%, 20% and 10%. For the larger system (shown as "L" in the chart legend), only the case of 30% functional group is studied.

aggregation, which can adversely affect the interaction force between DOX and ND.[1]

Nevertheless, our study clearly suggests that pH is a critical factor to DOX interaction with ND. This work paves the way for the continued and optimized development of a pH controlled drug delivery method using ND carriers.

AUTHOR INFORMATION

Corresponding Author

*W.K.L.: Northwestern University, Department of Mechanical Engineering, 2145 Sheridan Road, Evanston, IL 60208-3111, United States; tel, +1-847-491-7094; fax, +1-847-491-3915; e-mail, w-liu@northwestern.edu.

Notes

○ Walter P. Murphy Professor of Mechanical Engineering.

ACKNOWLEDGMENT

Financial Support from the US National Science Foundation (Grant CMMI-0856492) is greatly appreciated. W.K.L. acknowledged the partial support of the World Class University program (R33-10079) under the Ministry of Education, Science and Technology, Republic of Korea. D.H. gratefully acknowledges support from a National Science Foundation CAREER Award (CMMI-0846323), V Foundation for Cancer Research V Scholars Award, National Science Foundation Center for Scalable and Integrated NanoManufacturing (SINAM) Grant DMI-0327077, and Wallace H. Coulter Foundation Early Career Award in Translational Research. A.S.B. acknowledges support from the Australian National Computational Infrastructure (NCI) national facility under Grant q27.

REFERENCES

(1) Huang, H.; Pierstorff, E.; Osawa, E.; Ho, D. Active Nanodiamond Hydrogels for Chemotherapeutic Delivery. *Nano Lett.* **2007**, *7*, 3305–3314.

(2) Huang, L. C.; Chang, H. C. Adsorption and Immobilization of Cytochrome c on Nanodiamonds. *Langmuir* **2004**, *20*, 5879–5884.

(3) Shimkunas, R. A.; Robinson, E.; Lam, R; Lu, S.; Xu, X.; Zhang, X.-Q.; Huang, H.; Osawa, E; Ho, D. Nanodiamond-insulin complexes as pH-dependent protein delivery vehicles. *Biomaterials* **2009**, *30*, 5720–5728.

(4) Chen, M.; Pierstorff, E. D.; Lam, R.; Li, S.-Y.; Huang, H.; Osawa, E.; Ho, D. Nanodiamond-Mediated Delivery of Water- Insoluble Therapeutics. *ACS Nano* **2009**, *3*, 2016–2022.

(5) Liu, K. K.; Cheng, C. L.; Chang, C. C.; Chao, J. I. Alpha-bungarotoxin binding to target cell in a developing visual system by carboxylated nanodiamond. *Nanotechnology* **2007**, *18*, 10–16.

(6) Schrand, A. M.; Dai, L.; Schlager, J. J.; Hussain, S. M.; Osawa, E. Differential biocompatibility of carbon nanotubes and nanodiamonds. *Diamond Relat. Mater.* **2007**, *16*, 2118–2123.

(7) Barnard, A. S. Self-assembly in Nanodiamond Agglutinates. *J. Mater. Chem.* **2008**, *18*, 4038–4041.

(8) Barnard, A. S.; Sternberg, M. Crystallinity and Surface Electrostatics of Diamond Nanocrystals. *J. Mater. Chem.* **2007**, *17*, 4811–4819.

(9) Osawa, E.; Ho, D.; Huang, H.; Korobov, M. V; Rozhkova, N. N. Consequences of strong and diverse electrostatic potential fields on the surface of detonation nanodiamond particle. *Diamond Relat. Mater.* **2009**, *18*, 904–909.

(10) Ranson, M. R.; Carmichael, J.; O'byrne, K.; Stewart, S.; Smith, D.; Howell, A. Treatment of advanced breast cancer with sterically stabilized liposomal doxorubicin: results of a multicenter phase II trial. *J. Clin. Oncol.* **1997**, *15*, 3185–3191.

(11) Allen, T. M.; Cullis, P. R. Drug delivery systems: Entering the mainstream. *Science* **2004**, *303*, 1818–1822.

(12) Myrdal, P. B.; Yalkowsky, S. H. In *Encyclopedia of Pharmaceutical Technology*; Swarbrick, J., Boylan, J. C., Eds.; CRC Press: Boca Raton, FL, 2002, pp 2458−2480.

(13) Zhang, X.-Q.; Chen, M.; Lam, R.; Xu, X.; Osawa, E.; Ho, D. Polymer-functionalized nanodiamond platforms as vehicles for gene delivery. *ACS Nano* **2009**, *3*, 2609–2616.

(14) Loh, O.; Lam, R.; Chen, M.; Moldovan, N.; Huang, H.; Ho, D.; Espinosa, H. D. Nanofountain-Probe-Based High-Resolution Patterning and Single-Cell Injection of Functionalized Nanodiamonds. *Small* **2009**, *5*, 1667–1674.

(15) Lam, R.; Chen, M.; Pierstorff, E.; Huang, H.; Osawa, E.; Ho, D. Nanodiamond-Embedded Microfilm Devices for Localized Chemotherapeutic Elution. *ACS Nano* **2008**, *2*, 2095–2102.

(16) Huang, H.; Pierstorff, E; Ho, D. Self-assembling Dispersed Detonation Nanodiamonds into a Biofunctional NanoFilm. *ACS Nano* **2008**, 203–212.

(17) Manus, L. M.; Mastarone, D. J.; Waters, E. A.; Zhang, X.-Q; Schultz-Sikma, E. A.; MacRenaris, K. W.; Ho, D.; Meade, T. J. Gd(III). Nanodiamond Conjugates for MRI Contrast Enhancement. *Nano Lett.* **2010**, *10*, 484–489.

(18) Kloss, F. R.; Gassner, R.; Preiner, J.; Ebner, A.; Larsson, K.; Hachl, O.; Tuli, T.; Rasse, M.; Moser, D.; Laimer, K.; Nickel, E. A.; Laschober, G.; Brunauer, R.; Klima, G.; Hinterdorfer, P.; Steinmuller-Nethl, D.; Lepperdinger, G. The role of oxygen termination of nanocrystalline diamond on immobilisation of BMP-2 and subsequent bone formation. *Biomaterials* **2008**, *29*, 2433.

(19) Steinmuller-Nethl, D.; Kloss, F. R.; Najam-U-Haq, M.; Rainer, M.; Larsson, K.; Linsmeier, C.; Koehler, G.; Fehrer, C.; Lepperdinger, G.; Liu, X.; Memmel, N.; Bertel, E.; Huck, C. W.; Gassner, R.; Bonn, G. Strong binding of bioactive BMP-2 to nanocrystalline diamond by physisorption. *Biomaterials* **2006**, *27*, 4547.

(20) Serr, A.; Horinek, D.; Netz, R. R. Polypeptide friction and adhesion on hydrophobic and hydrophilic surfaces: A molecular dynamics case study. *J. Am. Chem. Soc.* **2008**, *130*, 12408.

(21) Horinek, D.; Serr, A.; Geisler, M.; Pirzer, T.; Slotta, U.; Lud, S. Q.; Garrido, J. A.; Scheibel, T.; Hugel, T.; Netz, R. R. Peptide adsorption on a hydrophobic surface results from an interplay of solvation, surface, and intrapeptide forces. *Proc. Natl. Acad. Sci. U.S.A.* **2008**, *105*, 2842.

(22) Borisenko, K. B.; Reavy, H. J.; Zhao, Q.; Abel, E. W. Adhesion of protein residues to substituted (111) diamond surfaces: An insight from

density functional theory and classical molecular dynamics simulations. *J. Biomed. Mater. Res., Part A* **2008**, *86A*, 1113.

(23) Baptista, A. M.; Teixeira, V. H.; Soares, C. M. Constant-pH molecular dynamics using stochastic titration. *J. Chem. Phys.* **2002**, *117*, 4184–4196.

(24) Shenderova, O. A., Gruen, D. M., Eds. *Ultrananocrystalline Diamond: Synthesis, Properties and Applications of*; William Andrew Publishing: Norwich, NY, 2006.

(25) Henderson, L. J. Concerning the relationship between the strength of acids and their capacity to preserve neutrality. *Am. J. Physiol.* **1908**, *21*, 173–179.

(26) Hasselbalch, K. A. Die Berechnung der Wasserstoffzahl des Blutes aus der freien und gebundenen Kohlensäure desselben, und die Sauerstoffbindung des Blutes als Funktion der Wasserstoffzahl. *Biochem. Z.* **1917**, *78*, 112–144.

(27) Po, H. N.; Senozan, N. M. Henderson−Hasselbalch Equation: Its History and Limitation. *J. Chem. Educ.* **2001**, *78*, 1499–1503.

(28) Gibson, N.; Shenderova, A. O.; Luo, T. J. M.; Moseenkov, S.; Bondar, V.; Puzyr, A.; Purtov, K.; Fitzgerald, Z.; Brenner, D. W. Colloidal stability of modified nanodiamond particles. *Diamond Relat. Mater.* **2009**, *18*, 620–626.

(29) Elimelech, M.; Gregory, J.; Jia, X.; Williams, R. A. In *Particle Deposition and Aggregation: Measurement, Modeling and Simulation*; Butterworth-Heineman: Woburn, MA, USA, 1995.

(30) Case, D. A.; Darden, T. A.; Cheatham, T. E., III; Simmerling, C. L.; Wang, J.; Duke, R. E.; Luo, R.; Crowley, M.; Walker, R. C.; Zhang, W.; Merz, K. M.; Wang, B.; Hayik, S.; Roitberg, A.; Seabra, G;. Kolossváry, I.; Wong, K. F.; Paesani, F.; Vanicek, J.; Wu, X.; Brozell, S. R.; Steinbrecher, T.; Gohlke, H.; Yang, L.; Tan, C.; Mongan, J.; Hornak, V.; Cui, G.; Mathews, D. H.; Seetin, M. G.; Sagui, C.; Babin, V.; Kollman, P. A. *AMBER 10*; University of California: San Francisco, 2008.

(31) Tersoff, J. Modeling solid-state chemistry: Interatomic potentials for multicomponent systems. *Phys. Rev. B* **1989**, *39*, 5566–5568.

(32) Mayo, S. L.; Olafson, B. D.; Goddard, W.A., III. DREIDING: A Generic Force Field for Molecular Simulations. *J. Phys. Chem.* **1990**, *94*, 8897–8909.

(33) Allen, M. P.; Tildesley, D. J. In *Computer Simulations of Liquids*; Oxford University Press: New York, USA, 1987.

(34) Hoover, W. G. Canonical dynamics: Equilibrium phase-space distributions. *Phys. Rev. A* **1985**, *31*, 1695–1697.

(35) Menozzi, M.; Valentini, L.; Vannini, E.; Arcamone, F. Self-association of doxorubicin and related compounds in aqueous solution. *J. Pharm. Sci.* **1984**, *73*, 766–770.

(36) Speelmans, G.; Staffhorst, R.; Dekruijff, B.; Dewolf, F. A. Transport studies of doxorubicin in model membranes indicate a difference in passive diffusion across and binding at the outer and inner leaflets of the plasma-membrane. *Biochemistry* **1994**, *33*, 13761.